Low-resolution neuronal code: a theory

Running head: Low-resolution neuronal code: a theory

Dr Mike Gilbert (corresponding author)

m.gilbert.1@bham.ac.uk

School of Psychology, College of Life and Environmental Sciences, University of Birmingham B15 2TT, UK

ORCID: 0000-0003-4415-6915

Dr Anders Rasmussen

Address: Department of Experimental Medical Science, Lund University, BMC F10, 22184 Lund, Sweden

ORCID: 0000-0003-4477-369X

ABSTRACT

It is a long-standing puzzle how insentient brain structures work 'blind', that is, seemingly with little or no information about the data they process. A plausible solution may be that, in some cases, they work in low resolution, i.e., sacrifice detail by disregarding it. That way, there is no need to read individual signals (respond in a way that reflects source and modality, for example). This feels counterintuitive because it seems wasteful, and also because it challenges the assumption that detail is desirable because it makes brain computations more powerful. Worse, physiological implementation faces problems. There must a threshold (data loss must be somehow limited or bounded), a way for lossy data to code information, a way to read it, a substrate and functional context. This is not a compromise but a strategy. The cerebellar cortex is a plausible substrate. The main source of excitatory input to the cerebellum, mossy fibres, terminate in the inner layer of the cerebellar cortex. We propose a neurophysiologically-detailed mechanism that recodes input to the cerebellum into internal signals. Resolution has spatial dimensions set by topography at the scale of long strips. The code is contained in collective parameters of firing rates, read by random sampling. We model the mechanism *in silico* to quantify and test the ideas. The detail of the hypothesis and the simulation is paramount because it is crucial that biological messiness at local scale does not compromise performance. We find that low-resolution code is an excellent candidate to explain cerebellar neurophysiology.

NEW AND NOTEWORTHY

It is a long-standing puzzle how brain structures work with so little information about the data they process. A seldom-considered but plausible solution is to work in low resolution, i.e., sacrifice detail by disregarding it. The problem *then* is to coordinate the behaviour of functionally-grouped cells which may individually receive an entirely different mixture of eclectic inputs. We propose a biologically-detailed mechanism which solves that problem and may have applications in other brain regions.

Keywords: theory, hypothesis, cerebellum, Golgi cell, code

1. Introduction

It is a long-standing theoretical problem how information is represented in joint activity of groups of neurons. It is another problem how cells which individually receive signals of mixed types, and each receive different signals, work together (to code information) in a concerted way. A low-resolution code – where the detail of the input 'picture' is discarded below a scale threshold – may in some cases provide a solution.

The largest source of glutamatergic input to the cerebellum is from mossy fibres, which contact granule cells in the inner layer of the cerebellar cortex, the granular layer. There is well-established fine-grain topography of input to the cerebellum which corresponds with its internal microcircuits (1-4). We hypothesised that within the boundaries of a topographically-defined region (long thin strips), information is indivisible. That is, finer resolution is not available to the cerebellum. Inside, signals are randomly intermingled. The input code is contained in statistical parameters of concurrent firing rates. Physiology is expressly adapted to be blind to other parameters (indeed, to block an effect, which would be noise). Random sampling below the resolution threshold, at local scale, provides the mechanism to read it. Random sampling has statistical effects. Given enough samples, statistics contained in input (mossy fibre) rates predict statistics contained in output (granule cell) rates.

In this way, rate information is conserved, eclectic input signals are converted to a normalised internal scale, and internal rates are constrained to a narrower range, with a distribution centred on the mean.

Below the topographically-set scale threshold, cells receive a random mix of multimodal inputs. A challenge for the low-resolution model is to explain, in that case, how they behave in a concerted way. Behaving concertedly – i.e., a group code – is a requirement self-imposed by sacrificing the resolution that would be needed to drive independent behaviour. We show a statistical code can deliver concerted behaviour. This – we suggest – underpins unitary behaviour of modular cerebellar circuits which is not explained by learning models.

These proposals have not previously been made, as far as we know. They are quantified by a simulation which is closely modelled on physiology, and accordingly supported by detailed evidence. The physiology of the cerebellum is strongly characterised by its modular wiring. The proposals explain the physiology of the entry node of the repeating cerebellar network. Entry-node recoding is an always-present and important part of cerebellar computations, and the cerebellum is a major brain structure. For these reasons, we hope it is of interest to the general neurophysiologist.

We cite neuroanatomy which has been known for years. We consider that anatomical evidence has been underused in theory. We think cell morphology and anatomical connectivity has a computational function. To explain how it implements that function

– and because it provides parameters and values that are used in the simulation – we describe and cite it.

The purpose of the simulation is to quantify and test the hypothesis. Part of the purpose of the test is to show that the mechanism works in physiological practice as opposed to only hypothetical principle. We claim anatomy exploits computational principles. Clearly, one could write code that does that, and works. That is not our approach. We closely replicate biological messiness – anatomical chance variability – on a detailed local scale, building up to a strip. We confirm that actual physiology, with all its random variables, is a viable substrate (and in fact even making simulated refinements to optimise performance don't improve it very much).

The main (functional, high-level) predictions of the hypothesis are that: i) conversion of input signals to internal signals generate internal signals in a narrowed frequency range with a distribution centred on the mean (focused bandwidth, tending-to-normal distribution); ii) parameters of input firing rates – rate statistics – predict certain statistics of internal firing rates (rate information is conserved in a collective internal code); and iii) by accepting data loss, the internal code has spatial dimensions which the cerebellum is able to dictate (it spans the cerebellar network – below that scale, information is indivisible). The simulation confirmed these predictions in the conditions tested.

An unpredicted finding was that there is an inherent level of noise (input never *perfectly* predicts output – there is always residual uncertainty in a small range). We had expected that, in a simulated system, output could be made progressively more precise, and ultimately very precise, by making refinements to the mechanism. In fact, there is a modest and diminishing return of making unphysiological improvements, and noise cannot be eliminated.

The rate code is not the only output of the granular layer conversion. Recoding also regulates the number of outputs. A second unpredicted finding was that sparse output is less noisy – a low number is more stable (less variable by chance given the same inputs). Regulation of the number of outputs – so that the volume of internal signals traffic is held at a low (5) or fixed (6) level – has long been thought to be an important function of recoding. However, it was generally assumed that regulation would involve a feedback loop that passes through the outer layer of the cerebellar cortex, the molecular layer. We found the granular layer is a potentially effective regulator on its own.

Cerebellar theory is dominated by supervised learning models (7-10). In those models, the granular layer provides a pre-processing stage (11). Output of pre-processing is passed to the main stage, whose function is long-term modification of synaptic weights by training. Following training, the naive response to signals in a pattern received by modified synapses is displaced by a learned response. We have discussed learning

models previously (see in particular (12, Discussion)). We think learning models are wrong. This paper is part of a set of proposals which present an alternative model (13, 14) which does not include a machine learning algorithm and in which recoding is not ancillary to a later stage. Instead, there is no functional priority of stages (network layers). Simply, they cooperate, each in a different role. Our scope in this paper is the input layer of the network – the conversion of mossy fibre input to the cerebellum into internal signals. Since we only look at the input layer there is, strictly speaking, no need here to challenge the traditional model. We raise it to explain why we don't discuss – for example – how output of recoding might be passed to or combined with learning models.

The next two sections provide a grounding in physiology, reflecting its central importance to the model.

2. Fields and Golgi cell ensembles

2.1 Fields (and ranks) defined

We use notional 'fields' to quantify some of the ideas. The cerebellar cortex is divided functionally (but not anatomically) into long thin strips termed microzones. Mossy fibres travel mediolaterally (the direction of the axis of folia), giving rise to sagittally-extending branches (the direction of the long axis of microzones) which terminate in the granular layer, on granule cells. A branch gives rise to several clusters of terminals (Figure 1). Terminal clusters are strictly aligned sagittally and separated by a variable

distance typically not less than 200 µm (15-17), (more from centre to centre of clusters).

There is to date no evidence of organisation of mossy fibre termination inside a sagittal strip. While termination of mossy fibres conforms topographically with fine-grained microzonal organisation of the cerebellar cortex, on a smaller scale terminals are intimately and randomly intermingled with terminals of other mossy fibres, and target selection is at random.

So, mossy fibres do not terminate at a point but a region with dimensions: the field occupied by a terminal cluster. Cluster size is variable (because it depends on the number of terminals and how tightly clustered they are), averaging 200 µm sagittally x 150 µm mediolaterally (16). 'Field' will be used to mean a region with these dimensions. This has the useful feature that a sagittal row of 75–100 fields has about the dimensions (in those directions) of a microzone. Microzone dimensions vary, but a mediolateral span of 150 µm is mid-range (3, 10, 18, 19). A row of 100 field will be termed a 'rank'.

Figure 1 about here

2.2 Golgi cell ensembles defined

Golgi cells are large interneurons whose cell bodies lie in the granular layer, where they inhibit granule cells. Mossy fibres make contact on Golgi cell basal dendrites in a structure termed a glomerulus (20-22), which is ensheathed in a semi-permeable

membrane. The glomerulus is also where mossy fibres excite granule cells and Golgi cells inhibit them. Mossy fibres therefore directly excite granule cells and inhibit them through Golgi cells, sometimes termed the feed-forward pathway. Golgi cells provide the only inhibitory input to granule cells. Most of the Golgi cell axonal plexus – which is confined to the granular layer – is made up of very fine beaded fibres. These enter glomeruli, where they contact granule cell dendrites (21) but the large majority of inhibition (98%) (23) is by spillover via $GABA_A$ receptors located perisynaptically and extrasynaptically (24, 25).

We will make a physiological and computational argument that functionally-grouped Golgi cells convert mossy fibre rates received by the group into self-regulating synchronised inhibition of granule cells. A functional group, or ensemble, occupies a sagittal row of three fields. The function of this arrangement is to synchronise modulation of GABA concentration across the glomerulus population of the middle field, and therefore synchronise inhibition of granule cells.

The rationale for ensembles is the same as for fields: they are nominal divisions of seamless anatomy which we use to quantify proposals.

4-5 Purkinje cells fit in a field, based on an estimate of the number that span a microzone (10). Estimates of the ratio of Golgi cells to Purkinje cells vary. ‘In man, the ratio [of Purkinje cells to Golgi cells] is 1:1.5, while in the monkey and cat it is almost

1:1.9 and in the rat 1:3.3' (26). We will take it that there are 10 Golgi cells per field, a ratio of 2:1 with 5 Purkinje cells.

The Golgi cell axon branches profusely, giving rise to a dense plexus. The axonal field is sagittally elongated, that is, in the direction of the long axis of a microzone – mean range 650 +/- 179 µm by 180 +/- 40 µm (in mice: 27) – and is the depth of the granular layer, which it fills vertically.

Their density (28) and large, profusely ramified axonal field (27) means that Golgi cell axonal territories overlap extensively. So highly ramified is the Golgi cell axonal plexus that it appears cloudlike in images. We take it that a granule cell may be inhibited with equal probability by any of the Golgi cells whose territories overlap at that location, and indeed each of its dendrites may be inhibited by a different subset of Golgi cells. A single Golgi cell contacts thousands of granule cells (21). Unitary recordings confirm that a granule cell receives inhibition from multiple Golgi cells (29).

As Golgi cell axonal territories are sagittally elongated, they overlap more in that direction. In a sagittal row of three fields, the middle field is innervated by Golgi cells in that field and by Golgi cells in the two neighbouring fields. Those cells constitute the 'ensemble' afferent to the middle field. As axonal territories are three times as long as they are wide, there is – relatively – modest incursion from mediolaterally neighbouring Golgi cells.

3. Golgi cells conserve rate information

Our hypothesis is that ensembles convert mossy fibre rates received as input to three fields into synchronised inhibition of granule cells in the middle field. For that, there must be a computational relationship, so that input rates predict output. And for *that*, Golgi cell physiology must support high-fidelity transmission – rate information received as input must be conserved. Is there evidence for that?

Golgi cells fire autonomously. On a cautionary note, 'anaesthesia has a strong influence on spontaneous activity of Golgi cells' (30). Under anaesthesia, firing falls into a slow oscillating pattern (31). Under excitatory synaptic input, this disappears (32). Discharge at low rates with irregular timing under anaesthesia (33) is at higher rates with relatively regular timing without it (34-36).

Contact on Golgi cells by mossy fibres is multi-synaptic (22), contributing to a reliable, rapid (submillisecond) response (low quantal release per synapse but collectively low uncertainty). The fast rise time and weak distance dependence of the amplitude and timing of Golgi cell EPSCs evoked by mossy fibre signals, suggests that basal dendrites introduce relatively little filtering (37, 38), as expected for large-diameter dendrites.

A slow decay component associated with transmission by spillover is weak or absent, suggesting (unlike mossy fibre transmission to granule cells) a modest spillover component of transmission. Possible reasons are individually modest release probability (39) and lower-affinity AMPA receptors (40). Golgi cell 'firing frequency

increases linearly with the amplitude of depolarising current' (41 abstract). 'Sensory-evoked Golgi-cell inhibition [of a granule cell] scales proportionally with the level of mossy fiber excitatory synaptic input' to the same cell, such that inhibition reliably conveys mossy fibre rate information (29).

'Golgi cells can follow peripheral signals in a continuous fashion modulating their frequency with the intensity of the stimulus [citing (34, 35)]' (42). As a result, during movement, the 'output of Golgi cells varies smoothly as a function of input.…They are capable of modulating their output to reflect their input with little noise or signal distortion' (43).

So: mossy fibre rate information is conserved proportionally in Golgi cell firing rates.

4. Computational transformation by the Golgi cell ensemble

4.1 The hypothesis

Neural code has more than one physiological form. The form may change from layer to layer of a network (in addition to intracellular transitions). In the sequence of transitions through a Golgi cell ensemble, from mossy fibre rates to inhibition of granule cells, the form changes several times. We assume there is a proportional conversion at each step of the ensemble conversion. We make that assumption because it is the most likely explanation of the proportional relationship of input and output. This allows us to quantify information that takes different forms on a common

scale. Put another way, we do not need to *show* there is proportionality (because it is reported), but only explain it.

We argue in this section that ensembles exploit a statistical effect of random sampling. Ensembles perform better than single cells because there are more layers of sampling and more samples per layer.

Say a population of values (with any frequency distribution) is randomly sampled. There are n samples, sample size m. If we take the mean (or sum) of each sample, and n is large, the sample means have a normal or near-normal distribution, by the central limit theorem. (This works even if m is a range.)

The quality of the distribution depends on the size of the values n and m. A modest value of either or both gives an untidier distribution. However, a messy distribution gets tidier and more normal-looking if it is then itself randomly sampled, and the process is repeated.

To apply that to Golgi cell ensembles, the first-sampled population is of mossy fibre rates received by three fields. Three fields contain a total of 30 Golgi cells. Rates are sampled by Golgi cell basal dendrites. Say five basal dendrites arise from the Golgi cell soma (it is 4-6), the number of samples is 30 x 5 = 150. Sample size is the number of mossy fibres which make contact per dendrite. The number of mossy fibres which directly contact a Golgi cell is unreported. It has been estimated that a Golgi cell

‘cannot receive more than 10–12 MF [mossy fibre] inputs, given the total basolateral dendrites length and the density of glomeruli’ (30).

This sounds low for these reasons. Golgi cell dendrites extend radially and downwards, penetrating the granular layer deeply. A field contains 700 mossy fibre terminals – derived from estimates that 100 mossy fibres innervate a field, and that branch endings average ~7 terminals per cluster (16). By our estimate, 700 terminals and the range of a Golgi cell dendritic territory puts a single Golgi cell in range of contact by significantly more than 10–12 terminals, even substantially more. We take the number as 20 divided equally between five dendrites, so that m = 4. Sampling of mossy fibre rates is at random and independent of other dendrites, even dendrites of the same Golgi cell.

The mossy fibre activity signature during behaviour in freely-moving animals – a high fraction are active, many continuously (Supplementary Materials 1) – would suggest that in motor circuits Golgi cells receive time-varying but sustained input signals. Accordingly, unlike usual experimental conditions, dendritic signals are not discrete, but rather the modulation of a state of sustained depolarisation.

The postsynaptic result – charge transfer to the Golgi cell soma – is a function of input rates. Otherwise, it would not convey rate information. As far as we know, there are no data for transformation of *multiple* mossy fibre input rates into Golgi cell basal

dendritic depolarisation. We assume that depolarisation is a function of the mean of input rates. (The sum of rates also works.)

Taking the mean of random samples (the output of the dendrite function for each dendrite) creates a new set of values. The frequency distribution of the new values is in a more condensed range and centred on the mean.

Basal dendrites are 'tapering prolongations of the soma' (22 p.113). As dendritic charge transfer is passive, we might expect the rate of transfer from each dendrite to the soma is proportional to the potential difference between dendritic and somatic charge. Other things being equal, that creates a relatively straightforward computational relationship. Integration of dendritic states at the Golgi soma is represented by taking the mean of dendritic charge, that is, averaging the sample means for each cell.

This generates a third population of values – the outputs of the integration function. We assume (because rate information is reported to be conserved) there is a proportional conversion of somatic depolarisation to Golgi cell firing rates, and also (because of the profuseness of Golgi cell axonal branching) that each glomerulus receives input from a random sample of Golgi cells afferent to a field. Here also, rates are randomly sampled. Sample size is the (unknown, as far as we are aware) number of Golgi cells with convergent input to a glomerulus, and the number of samples is the number of glomeruli per field.

It has been suggested there may be a sustained build-up of glomerular GABA during behaviour (44) at an adjustable concentration controlled by Golgi cell firing rates (45). The concentration of GABA, and therefore Inhibition of granule cells, may receive modulation from another source as well, however. Intraglomerular GABA concentration receives modulation in a dynamic balance with glumatate. Activation of presynaptic $GABA_B$ receptors on mossy fibres inhibits glutamate release (46), while activation of presynaptic mGluR2 receptors on Golgi cells inhibits GABA release (47). This may create a positive feedback loop, where either glutamate or GABA prevails. The result seems to be a glomerulus-by-glomerulus competition for influence with an outcome that is independent of other mossy fibre terminals, even other terminals that provide input to the same granule cell.

We take the output of the ensemble conversion to be the mean of Golgi cell rates received individually by each glomerulus in a field (so there are 700 outputs per field, because there are 700 glomeruli). The mean of Golgi cell rates received by a glomerulus is the 'rate threshold'. The mossy fibre signal received by a glomerulus must exceed the rate threshold to prevail in the glomerular competition. Only mossy fibre signals that prevail depolarise a granule cell.

Figure 2 about here

4.2 Simulation of the Golgi cell ensemble conversion

4.2.1 Feed-forward inhibition of a field is synchronised

Mossy fibre firing rates received by a rank were simulated with the distributions shown in Figure 2, column 1. The frequency distribution of firing rates received by a row of three fields selected at random is shown (in red) in the same panel. Each field receives a random sample of rates received by the rank as a whole. Terminal clustering means a field receives copies of most signals, so to represent *signals* received by a field, as opposed to *rates*, copies need to be added. 100 mossy fibres innervate a field taken as a proportionate fraction of the number that innervate a larger area (16). As fields are the size of an average-sized terminal cluster, and we take the mean as 7 (it is 7–8), the total number of terminals per field is 700, the maximum number of copies of a signal is 7, and the mean number is 4.

The actual number of mossy fibres afferent to a field is higher because many clusters straddle nominal field boundaries, so a larger number of cells is needed to make up the number of terminals inside. At the local level – field scale – anatomical variables increase uncertainty. The simulation uses an algorithm so that sampling (including sample size), and adding copies, reflects biological parameters (Supplementary Materials 2). We estimate the number of mossy fibres afferent to a field (and therefore sample size) is ∼180.

We assume that a rank receives on average 5 terminal clusters per mossy fibre. The number of mossy fibres afferent to a rank is the product of the number afferent to a field and the number of fields in a rank, divided by the average number of terminal branches per mossy fibre, giving 3,645 (given a rank of 100 fields).

Therefore, although 100 fields fit in a rank, the number of *signals* received by a field is ∼19% of the *rates* received by a rank, and the number received by 3 fields is ∼57%.

Some very high mossy fibre rates can be generated in experimental conditions. However, it is thought the typical physiological range is 50–300 Hz (48) citing (49). In the simulations, rates are generated at random in that range, within constraints on the distribution. The constraints depend on the shape of the distribution.

Mossy fibre terminal branching means a mossy fibre signal is typically received by multiple fields. Physiologically, there is a cap on the number of fields that can receive a signal, because it is limited to the number of branch endings of the cell. There is no cap in the simulation but the number of repeat samplings of a signal in the simulation is statistically limited so that it reflects the physiological number of branch endings (Supplementary Materials 3).

In Figure 2 column 2, the red data are themselves randomly sampled – 150 samples, sample size 4, representing 30 Golgi cells x 5 basal dendrites, and contact on each dendrite by 4 mossy fibres – and the sample means plotted, representing dendritic charge states. The range is narrower than the sampled population (in all rows), but

data are not tightly grouped. (NB. values in this and the next step are proportional to charge, on a proxy scale.)

In column 3, the sample means are themselves sampled – 30 samples, sample size 5, representing 30 Golgi cells with 5 dendrites each – and the samples averaged (and plotted), representing somatic charge states. Somatic data are in a narrower range than dendritic data but still not tightly grouped.

In the final step (column 4) somatic data are sampled 700 times, sample size 8–12, reflecting convergent input from 3 fields of Golgi cells onto 700 glomeruli in the middle field, with an assumed (because it is unknown) convergence ratio of 8–12:1. Column 5 shows the column 4 data as a histogram, for comparison with column 1.

The result in all rows is that mossy fibre signal frequencies received as input to a rank are reliably converted to a narrow distribution of values representing inhibition of granule cells. The transformation is striking, consistent with the evidence, and it works for any distribution of mossy fibre rates, although a narrower input distribution returns a narrower output distribution.

Our findings are:

i) In the tested conditions, the hypothesised ensemble mechanism generated the expected results; mossy fibre rates are converted to a well-synchronised field-wide rate threshold;

ii) Golgi cells work together; ensembles represent a minimum functional scale.

Figure 3 about here

4.2.2 Unknown parameters

We next explored the effect of varying model parameters for which physiological data are unreported. We did that to verify that the conversion is not critically dependent on ratios that have not been reported, which we surmise in the simulation.

Figure 3a and b show the results. In 3a, the varied parameter is the number of mossy fibres with convergent input to a single Golgi cell dendrite, and in 3b, the number of Golgi cells with convergent input to a glomerulus. The plotted data in both cases represent the mean of convergent Golgi cell rates received by each glomerulus in the middle field of a simulated ensemble (so 700 values, the same as Figure 2, column 4). In both cases, increasing the convergence ratio condenses the plotted data range (representing tighter alignment within a field), but there is a diminishing return. There is a stronger effect of increasing a low ratio and a progressively weakening effect at higher ratios. The conversion mechanism is robust across most of the range of values for unreported parameters. Only a very low Golgi cell to glomerulus ratio caused a wide spread of the data.

NB. In other panels and other figures, ratios are 4:1 (mossy fibres that contact a Golgi cell basal dendrite) and 8–12:1 (Golgi cells that converge on a glomerulus). Both are

towards the low end of the possible range, intended to be conservative (i.e., not selected because they are favourable – or unfavourable – to the hypothesis).

A second finding was that input and output of an ensemble were independently variable below a scale threshold. Input was taken as the mean of mossy fibre rates received by a row of three fields (with copies added). Output was taken as the mean of rate thresholds in the middle field (i.e., derived by calculating the mean of Golgi cell rates received by each glomerulus in the middle field, then taking the average: the 'glomerulus field mean'). They both varied in approximately the same range (which was proportional to variance of the sampled distribution), but within that range they varied at random and independently. Independence was the result of random sampling by Golgi cells of mossy fibre rates. There was no effect of random sampling by glomeruli of Golgi cell rates (the glomerulus field mean moves relative to the mean of mossy fibre rates in the left 4 panels, where mossy fibre rates are resampled in every panel, and not in the right 4 columns).

Figure 4 about here

4.2.3 Feed-forward inhibition of a rank is synchronised

We explored the reason for variation of excitation and inhibition of a field relative to each other in Figure 4. Excitation was taken as the mean of mossy fibre rates with copies added (the 'MF field mean'). Inhibition was taken as the glomerulus field mean.

The middle column shows the mean of mossy fibre rates received by each field in a row of 50, with and without copies added. (We simulated 100 fields but show 50 to improve presentation.) The right column shows the copies-added mossy fibre data and glomerulus field means, again for 50 fields.

In the middle column, red data (MF field means) closely track the yellow data (the same, but without copies added), indicating that adding copies does not skew the mean of firing rates received by a field.

In the right column, the red (MF field means) and blue (glomerulus field means) data vary randomly from field to field and relative to each other. The shortened range of the y axis belies the same contraction of the data range compared to the sampled distribution seen in Figure 2. In rows 4b and 4d, the SD of the glomerulus field means is ~3 Hz, derived from mossy fibre rates with a range of ~160 Hz, SD 25 Hz.

Within that, however, the output of the ensemble conversion (the glomerulus field means) is variable by chance. We tested if there is an effect on the range caused by unknown convergence ratios. In rows 4c and 4d we set convergence ratios 'optimally' for mossy fibres onto a Golgi cell and for Golgi cells onto a glomerulus (i.e., both are set at 24:1). This did not reduce the range of variation of the glomerulus field means or reduce field-to-field variation (there is a modest effect, but it depends on the shape of the sampled distribution, and it is inconsistent).

Our findings are:

i) Field-to-field variability of the MF field means is the result of random sampling of mossy fibre rates (and not adding copies);

ii) The reason for field-to-field variation of the glomerulus field means is the effect of chance inherent in random sampling, in this case as part of the mechanism of the ensemble conversion. It is an artefact of the mechanism as opposed to necessarily being poor performance.

iii) The mean of mossy fibre rates received by a field and mean inhibition received by glomeruli in that field vary at random and independently (in a limited range), both the effect of chance inherent in random sampling. Variability is not compounded – the effect of layers of random sampling is not cumulative.

iv) The glomerulus field means (the output of the ensemble conversion), averaged across fields in a rank, have a linear relationship with the mean of the sampled distribution (input to the rank). That is, subject to (ii), inhibition of granule cells is synchronised in a rank: Golgi cells work together in functionally unitary sagittal strips.

To gauge if that effect is functionally significant – that is, if it impacts wider performance metrics – in the next section we incorporate the Golgi cell ensemble conversion into a simulation of the mechanism that converts mossy fibre signals into granule cell signals.

Figure 5 about here

5. Neurophysiology implements a computational conversion of mossy fibre rates into granule cell signals

We incorporated the Golgi cell ensemble conversion into a simulation of recoding in the granular layer. The mechanism provides a functional explanation of granular layer neurophysiology. Part of the explanation is that anatomy exploits statistical effects. Some of the ideas first appeared here (50). The next section extends the physiological argument made for the Golgi cell ensemble conversion, and in Supplementary Materials 1–3.

5.1 The physiological basis for the recoding mechanism: the hypothesis

Granule cells receive input to each dendrite from a single mossy fibre. If (as it seems) contact by mossy fibres on granule cells is at random, a granule cell is very likely to receive input from a different mossy fibre to each of its dendrites (Supplementary Materials 4). Granule cells which populate a field each receive as input a random sample of mossy fibre firing rates received is input to that field, sample size 3–5 (the number of granule cell dendrites). More accurately, they receive a random sample of *signals*, reflecting the fact that a field receives a variable number of copies of most rates. The simulation samples signals but, as noted, the chances that a granule cell receives contact twice from the same mossy fibre are remote. The simulation assumes all granule cells have 4 dendrites, the average (51) (the outcome is the same with 3–5).

To recap, each mossy fibre terminal is surrounded by a semi-permeable sheath that restricts neurotransmitter diffusion – the glomerulus. Mossy fibres excite Golgi cells, and Golgi cells inhibit granule cells. Excitation of Golgi cells by mossy fibres is largely synaptic with a modest spillover component (22, 39, 40). By contrast, inhibition of granule cells by Golgi cells is largely through spillover with a small synaptic component (24, 25, 52). In each glomerulus, excitation and inhibition compete for influence. It is unclear if there is always an emphatic winner, but it is possible, because GABA inhibits glutamate release (46) and glutamate inhibits GABA release (47), so that a swing in the dominant direction may be amplified by positive feedback.

A granule cell needs a minimum number of active mossy fibre inputs to fire – thought to be three (48, 53). Certainly, one is too few (23, 54, 55). We take it as three, and call it the granule cell 'input threshold'. Three signals is not in itself sufficient, as each of those signals must also prevail in the glomerular competition. We assume that to count towards the input threshold, mossy fibre signal frequency must exceed a threshold. Weak signals have no effect. The threshold is provided by the Golgi cell ensemble conversion.

5.2 Simulation of granular layer recoding

We randomly sampled values representing mossy fibre firing rates received by a rank to represent firing rates received by each field in a row of 100, then used the recoding

mechanism to turn that into a number of granule cells that fire in each field, and the firing rates they each receive as input.

The output of the Golgi cell ensemble conversion is inhibition which provides the rate threshold. As discussed, there are 700 outputs of the ensemble conversion per field, one for each glomerulus. Inhibition of a field is synchronised, that is, in a narrow range, but within that range it varies at random. Each glomerulus receives a different pairing of excitation and inhibition.

The program compares mossy fibre signal frequency with the rate threshold at each of 4 dendrites of each of 8,750 granule cells in each of 100 fields, assuming that granule cells randomly sample mossy fibre rates. It takes the mean of the rates received by each granule cell (the sample means), identifies the subset that fire (cells that receive at least 3 mossy fibre signals which exceed the rate threshold), then takes the mean of the sample means for that subset, for each field.

5.3 Results

The results are shown in Figures 5 and 6.

i) The shape of the frequency distribution of the granule cell sample means is coarsely symmetrical around the mean of the distribution (the 'GC field mean'.) The spread of data is substantially narrowed compared to the sampled distribution (mossy fibre rates).

ii) As hypothesised, the GC field means have a linear relationship with the mean of the sampled distribution, if other parameters of the sampled distribution are fixed (Fig 6a–c). If the relationship was perfectly precise, the GC field means, plotted for each field in a rank, would be a straight horizontal line. In the simulation it is not straight, but the data are in a narrow range, and in some cases a very narrow range (depending on the frequency distribution of mossy fibre rates).

iii) This relationship holds even when a small percentage of granule cells are active (sub 1%) (Fig 5 rows 4–6 and Fig 6).

iv) The number of granule cells that fire is more stable at low numbers (Fig 5 right column). There is a clear effect even of reducing an already low number (sub 1%).

v) The effect of chance on Golgi cell ensemble output, inherent in the ensemble mechanism, do not compromise the recoding mechanism.

Figure 6 about here

5.4 Granule cell ascending axon feedback may enhance self-regulation

Chance variation of a low number of active granule cells is modest but still present. Sparse code therefore carries the risk that in some fields the number is too low to faithfully conserve rate information (if it is coded as statistics). Fine regulation of the number may be improved by feedback via granule cell ascending axon contact on Golgi cells (not included in the simulation).

Granule cells make ascending axon contact on Golgi cell basal dendrites (38). A Golgi cell receives ~400 functional synaptic contacts from this source, around 25% of the granule cells that a Golgi cell receives contact from in total. 'During sustained mf [mossy fibre] discharge, synapses from local GrCs [granule cells] contribute equivalent charge to GoCs [Golgi cells] as mf synapses' and 'display similarly fast kinetics' (56), providing the substrate for potent – local – inhibitory feedback. This may contribute to fine regulation of the number of active granule cells.

6. Discussion

We hypothesised that the cerebellum converts high-dimensional mossy fibre input into a low-dimensional internal code, and that this can explain the detailed physiology of the entry node of the modular cerebellar network. Our proposals include the spatial dimensions of resolution, the mechanism of conversion and the form of the internal code. We quantified and tested the proposals with computer models that very closely simulate neurophysiology, including random variability of individual cell anatomy. The purpose of the test was to confirm that granular layer architecture could plausibly implement the ideas, and that real world biological messiness does not mean it would not work.

We show plausibly that Golgi cells work together as functional units – ensembles. The function of ensembles, acting through the feed-forward pathway, is to convert mossy fibre input to a 3-field strip into synchronous inhibition of granule cells in the middle

field. The function of inhibition is to participate in recoding of mossy fibre signals into granule cell signals. Ensembles are not discrete but represent a minimum functional scale. Input to an ensemble-sized section of a rank is a random sample of mossy fibre rates received by the rank as a whole. As this can be *any* 3-field section, inhibition is synchronised between fields in a rank. The ensemble conversion can be inserted into a model of recoding that both regulates the number of granule cells that fire and reliably converts statistical parameters collectively coded in mossy fibre rates into a well-predicted granule cell code.

Since at any moment all fields randomly sample the same population of mossy fibre rates, and receive synchronised inhibition, they all return the same output code, as one. Just as input to a rank is the smallest unit of resolution, so is output: input is converted it to an internal form with the same dimensions. This happens through the action of a plausible substrate for which there is detailed evidence.

The smallest unit of resolution it is not the smallest unit of code. The internal code is contained in parameters of concurrent firing rates – rate statistics. Therefore, it is unnecessary to receive all output signals in order to read it, because it is coded in any (randomly sampled) much smaller number of signals, provided the sample is large enough for rate statistics to be present. That feature means it is independently readable downstream by small sections of a microzone, and also that all sections receive the same code.

The frequency distribution of the internal code is strongly narrowed compared to the sampled distribution. Narrowing is functional, we suggest, the first stage in a sequence that distils a single output rate of the network from many input rates. The uncomplicated reason may be that the cerebellar modular network participates in what remains at root a sensory-motor loop. There is no reason that this needs to include graduated synaptic weights or a learning algorithm. In this scenario, input rates control (vs merely drive) output. The challenge then is to *conserve* input rate information, through a (short) chain of recodings (there are two further network nodes) that convert many rates into one.

But with so many input rates, what is conserved? Conserved means simply: the output rate is faithfully predicted by input parameters, and perhaps only one – the mean of input rates, say. The unit of input data is a rank – a strip of the granular layer. The benefit of packaging input data into strip units is that it can represent a state, such as a changing state across the phases of a movement cycle, received from a body segment or a group of muscles, for example.

We have focused on control of Golgi cells by direct mossy fibre input. Golgi cells also receive granule cell input to dendrites which ascend into the outer layer of the cerebellar cortex, the molecular layer, which may contribute to regulation of the fraction of active granule cells (5, 6). Other possible inputs to Golgi cells are reviewed in Supplementary Materials 5.

It is a long-standing idea that cerebellar cortical architecture may implement computational workings. We propose a form that this may take in the granular layer. The mechanism can work with no information about input signals. This may explain how the cerebellum can work 'blind', except to the extent it is sighted by coarse topography. As the mechanism does not need to be adapted to the source or type of input, the cerebellum has been able to adopt a modular wiring plan.

Repeating circuit wiring is well preserved across species (57, 58). Modularity has allowed the vertebrate phenotype to diversify. By contrast, specialisation is repeatedly displaced from the gene pool. It may also be part of the reason that the cerebellum is good at adapting to lesions and damage – damaged circuits can be replaced from the unspecialised pool of anatomical raw material.

While we put strong emphasis on accounting for cerebellar physiology, some of the ideas presented here may be features of coding in other brain regions. A topographically-defined scale of resolution, random sampling below that scale, exploitation of statistical effects of random sampling, selected parameters of rate statistics that code information, and active blindness to other parameters, are examples.

Glossary

feed-forward inhibition Inhibition of granule cells by the pathway mossy fibre-Golgi cell-granule cell

field A 200 µm (sagittal) x 150 µm (mediolateral) area of the entry layer of the cerebellar cortex, the granular layer, the average dimensions of a mossy fibre terminal cluster.

GC field mean The mean, for each field, of the mean of mossy fibre rates received individually by active granule cells. A granule cell randomly samples mossy fibre rates; the GC field mean is the mean of the sample means, for the subset of granule cells that fire.

glomerulus field mean The mean, for each field, of the mean of Golgi cell rates received by each glomerulus in that field. A glomerulus randomly samples Golgi cell rates; the glomerulus field mean is the mean of the sample means.

input threshold The minimum number of mossy fibre signals (which exceed the rate threshold) that are needed to make a granule cell fire.

MF field mean The mean of mossy fibre rates (with copies added) received by a field.

rank A sagittal row of 100 fields; about the dimensions of a microzone. The reason we don't use 'microzone' is that a rank does not have to correspond to a microzone, it is a region only of the granular layer (whereas a microzone is defined by climbing fibre

input to the molecular layer), and while microzones do not have anatomical boundaries they are well-defined functionally, whereas a rank may have less definition.

rate threshold A measure of inhibition given by the average of Golgi cell rates received as convergent input to a glomerulus. A mossy fibre signal must exceed this value to count towards the granule cell input threshold.

Grants

Mike Gilbert was supported by a grant from the Leverhulme Trust (ECF-2022-079).

Anders Rasmussen was supported by grants from the Swedish Research Council (2020-01468), Per-Eric och Ulla Schybergs Foundation (42630), and the Crafoord Foundation (20180704, 20200729, 20220776, & 20230655).

Conflict of interest

The authors declare no conflicts of interest.

Author contributions

M.G. conceived and designed research; M.G. developed algorithms and wrote code; M.G. prepared figures; M.G. drafted manuscript; M.G. and A.R edited and revised manuscript; M.G. and A.R. approved final version of manuscript

REFERENCES

1. **Garwicz M, Apps R, and Trott JR**. Micro-organization of olivocerebellar and corticonuclear connections of the paravermal cerebellum in the cat. *The European journal of neuroscience* 8: 2726-2738, 1996.
2. **Garwicz M, and Ekerot CF**. Topographical organization of the cerebellar cortical projection to nucleus interpositus anterior in the cat. *The Journal of physiology* 474: 245-260, 1994.
3. **Garwicz M, Ekerot CF, and Jorntell H**. Organizational principles of cerebellar neuronal circuitry. *News in Physiological Sciences* 13: 28-34, 1998.
4. **Garwicz M, Jörntell H, and Ekerot CF**. Cutaneous receptive fields and topography of mossy fibres and climbing fibres projecting to cat cerebellar C3 zone. *The Journal of physiology* 512 (Pt 1): 277-293, 1998.
5. **Marr D**. A theory of cerebellar cortex. *The Journal of physiology* 202: 437-470, 1969.
6. **Albus JS**. A Theory of Cerebellar Function. *Mathematical Biosciences* 10: 25-61, 1971.
7. **Albus JS**. The Marr and Albus theories of the cerebellum-two early models of associative memory. In: *Digest of Papers COMPCON Spring 89 Thirty-Fourth IEEE Computer Society International Conference: Intellectual Leverage*1989, p. 577-582.
8. **Brunel N, Hakim V, Isope P, Nadal JP, and Barbour B**. Optimal information storage and the distribution of synaptic weights: perceptron versus Purkinje cell. *Neuron* 43: 745-757, 2004.
9. **Fujita M**. Adaptive filter model of the cerebellum. *Biological cybernetics* 45: 195-206, 1982.
10. **Dean P, Porrill J, Ekerot CF, and Jörntell H**. The cerebellar microcircuit as an adaptive filter: experimental and computational evidence. *Nature reviews Neuroscience* 11: 30-43, 2010.
11. **Raymond JL, and Medina JF**. Computational Principles of Supervised Learning in the Cerebellum. *Annual review of neuroscience* 41: 233-253, 2018.
12. **Gilbert M**. Gating by Memory: a Theory of Learning in the Cerebellum. *The Cerebellum* DOI: 10.1007/s12311-021-01325-9: 2021a.
13. **Gilbert M, and Miall RC**. Gating by Functionally Indivisible Cerebellar Circuits: a Hypothesis. *The Cerebellum* 20: 518-532, 2021b.
14. **Gilbert M**. The shape of data: A theory of the representation of information in the cerebellar cortex. *The Cerebellum* DOI: 10.1007/s12311-021-01352-6: 2021b.
15. **Wu HS, Sugihara I, and Shinoda Y**. Projection patterns of single mossy fibers originating from the lateral reticular nucleus in the rat cerebellar cortex and nuclei. *The Journal of comparative neurology* 411: 97-118, 1999.
16. **Sultan F, and Heck D**. Detection of sequences in the cerebellar cortex: numerical estimate of the possible number of tidal-wave inducing sequences represented. *Journal of physiology, Paris* 97: 591-600, 2003.
17. **Shinoda Y, and Sugihara I**. Axonal Trajectories of Single Climbing and Mossy Fiber Neurons in the Cerebellar Cortex and Nucleus. In: *Handbook of the Cerebellum and Cerebellar Disorders*, edited by Manto M, Schmahmann JD, Rossi F, Gruol DL, and Koibuchi N. Dordrecht: Springer Netherlands, 2013, p. 437-467.

18. **Oscarsson O**. Functional units of the cerebellum - sagittal zones and microzones. *Trends in Neurosciences* 2: 143-145, 1979.
19. **Ozden I, Sullivan MR, Lee HM, and Wang SS**. Reliable coding emerges from coactivation of climbing fibers in microbands of cerebellar Purkinje neurons. *The Journal of neuroscience : the official journal of the Society for Neuroscience* 29: 10463-10473, 2009.
20. **Eccles JC, Llinás R, and Sasaki K**. Golgi cell inhibition in the cerebellar cortex. *Nature* 204: 1265-1266, 1964.
21. **Hámori J, and Szentágothai J**. Participation of Golgi neuron processes in the cerebellar glomeruli: an electron microscope study. *Experimental brain research* 2: 35-48, 1966.
22. **Palay SL, and Chan-Palay V**. *Cerebellar cortex : cytology and organization*. Berlin: Springer, 1974.
23. **Duguid I, Branco T, London M, Chadderton P, and Hausser M**. Tonic inhibition enhances fidelity of sensory information transmission in the cerebellar cortex. *The Journal of neuroscience : the official journal of the Society for Neuroscience* 32: 11132-11143, 2012.
24. **Nusser Z, Sieghart W, and Somogyi P**. Segregation of different GABAA receptors to synaptic and extrasynaptic membranes of cerebellar granule cells. *The Journal of neuroscience : the official journal of the Society for Neuroscience* 18: 1693-1703, 1998.
25. **Brickley SG, Cull-Candy SG, and Farrant M**. Development of a tonic form of synaptic inhibition in rat cerebellar granule cells resulting from persistent activation of GABAA receptors. *The Journal of physiology* 497 (Pt 3): 753-759, 1996.
26. **Lange W**. Regional differences in the distribution of golgi cells in the cerebellar cortex of man and some other mammals. *Cell and tissue research* 153: 219-226, 1974.
27. **Barmack NH, and Yakhnitsa V**. Functions of interneurons in mouse cerebellum. *The Journal of neuroscience : the official journal of the Society for Neuroscience* 28: 1140-1152, 2008.
28. **Llinás RR, and Negrello MN**. Cerebellum http://www.scholarpedia.org/article/Cerebellum. [06/01, 2017].
29. **Duguid I, Branco T, Chadderton P, Arlt C, Powell K, and Hausser M**. Control of cerebellar granule cell output by sensory-evoked Golgi cell inhibition. *Proceedings of the National Academy of Sciences of the United States of America* 112: 13099-13104, 2015.
30. **Pietrajtis K, and Dieudonné S**. Golgi Neurons. In: *Handbook of the Cerebellum and Cerebellar Disorders*, edited by Manto M, Schmahmann JD, Rossi F, Gruol DL, and Koibuchi N. Dordrecht: Springer Netherlands, 2013, p. 829-852.
31. **Ros H, Sachdev RN, Yu Y, Sestan N, and McCormick DA**. Neocortical networks entrain neuronal circuits in cerebellar cortex. *The Journal of neuroscience : the official journal of the Society for Neuroscience* 29: 10309-10320, 2009.
32. **Vervaeke K, Lorincz A, Gleeson P, Farinella M, Nusser Z, and Silver RA**. Rapid desynchronization of an electrically coupled interneuron network with sparse excitatory synaptic input. *Neuron* 67: 435-451, 2010.
33. **Ruigrok TJ, Hensbroek RA, and Simpson JI**. Spontaneous activity signatures of morphologically identified interneurons in the vestibulocerebellum. *The Journal of neuroscience : the official journal of the Society for Neuroscience* 31: 712-724, 2011.
34. **Edgley SA, and Lidierth M**. The discharges of cerebellar Golgi cells during locomotion in the cat. *The Journal of physiology* 392: 315-332, 1987.

35. **Miles FA, Fuller JH, Braitman DJ, and Dow BM**. Long-term adaptive changes in primate vestibuloocular reflex. III. Electrophysiological observations in flocculus of normal monkeys. *Journal of neurophysiology* 43: 1437-1476, 1980.
36. **Rasmussen A, Zucca R, Jirenhed DA, Johansson F, Ortenblad C, Svensson P, and Hesslow G**. Golgi cell activity during eyeblink conditioning in decerebrate ferrets. *Cerebellum (London, England)* 13: 42-45, 2014.
37. **Kanichay RT, and Silver RA**. Synaptic and cellular properties of the feedforward inhibitory circuit within the input layer of the cerebellar cortex. *The Journal of neuroscience : the official journal of the Society for Neuroscience* 28: 8955-8967, 2008.
38. **Cesana E, Dieudonné S, Isope P, Bidoret C, D'Angelo E, and Forti L**. Novel granule cell-Golgi cell excitatory input in the cerebellar granular layer. In: *FENS Abstr*2010.
39. **DiGregorio DA, Nusser Z, and Silver RA**. Spillover of glutamate onto synaptic AMPA receptors enhances fast transmission at a cerebellar synapse. *Neuron* 35: 521-533, 2002.
40. **DiGregorio DA, Rothman JS, Nielsen TA, and Silver RA**. Desensitization properties of AMPA receptors at the cerebellar mossy fiber granule cell synapse. *The Journal of neuroscience : the official journal of the Society for Neuroscience* 27: 8344-8357, 2007.
41. **Dieudonné S**. Submillisecond kinetics and low efficacy of parallel fibre-Golgi cell synaptic currents in the rat cerebellum. *The Journal of physiology* 510 (Pt 3): 845-866, 1998.
42. **Galliano E, Mazzarello P, and D'Angelo E**. Discovery and rediscoveries of Golgi cells. *The Journal of physiology* 588: 3639-3655, 2010.
43. **Moore JW, and Blazis DEJ**. 11 - Simulation of a Classically Conditioned Response: A Cerebellar Neural Network Implementation of the Sutton–Barto–Desmond Model. In: *Neural Models of Plasticity*, edited by Byrne JH, and Berry WOAcademic Press, 1989, p. 187-207.
44. **Rossi DJ, Hamann M, and Attwell D**. Multiple modes of GABAergic inhibition of rat cerebellar granule cells. *The Journal of physiology* 548: 97-110, 2003.
45. **Mapelli L, Solinas S, and D'Angelo E**. Integration and regulation of glomerular inhibition in the cerebellar granular layer circuit. *Frontiers in cellular neuroscience* 8: 55, 2014.
46. **Mitchell SJ, and Silver RA**. GABA spillover from single inhibitory axons suppresses low-frequency excitatory transmission at the cerebellar glomerulus. *The Journal of neuroscience : the official journal of the Society for Neuroscience* 20: 8651-8658, 2000a.
47. **Mitchell SJ, and Silver RA**. Glutamate spillover suppresses inhibition by activating presynaptic mGluRs. *Nature* 404: 498-502, 2000b.
48. **Jörntell H, and Ekerot CF**. Properties of somatosensory synaptic integration in cerebellar granule cells in vivo. *The Journal of neuroscience : the official journal of the Society for Neuroscience* 26: 11786-11797, 2006.
49. **van Kan PL, Gibson AR, and Houk JC**. Movement-related inputs to intermediate cerebellum of the monkey. *Journal of neurophysiology* 69: 74-94, 1993.
50. **Gilbert M, and Miall RC**. How and Why the Cerebellum Recodes Input Signals: An Alternative to Machine Learning. *Neuroscientist* DOI: 10.1177/1073858420986795: 2021a.
51. **Eccles JC, Ito M, and Szentágothai J**. *The cerebellum as a neuronal machine*. Berlin, New York etc.: Springer-Verlag, 1967, p. 335 p.
52. **Hamann M, Rossi DJ, and Attwell D**. Tonic and spillover inhibition of granule cells control information flow through cerebellar cortex. *Neuron* 33: 625-633, 2002.
53. **Billings G, Piasini E, Lorincz A, Nusser Z, and Silver RA**. Network structure within the cerebellar input layer enables lossless sparse encoding. *Neuron* 83: 960-974, 2014.

54. **Chadderton P, Margrie TW, and Hausser M**. Integration of quanta in cerebellar granule cells during sensory processing. *Nature* 428: 856-860, 2004.
55. **Bengtsson F, and Jörntell H**. Sensory transmission in cerebellar granule cells relies on similarly coded mossy fiber inputs. *Proceedings of the National Academy of Sciences of the United States of America* 106: 2389-2394, 2009.
56. **Cesana E, Pietrajtis K, Bidoret C, Isope P, D'Angelo E, Dieudonne S, and Forti L**. Granule cell ascending axon excitatory synapses onto Golgi cells implement a potent feedback circuit in the cerebellar granular layer. *The Journal of neuroscience : the official journal of the Society for Neuroscience* 33: 12430-12446, 2013.
57. **Bell CC**. Evolution of cerebellum-like structures. *Brain, behavior and evolution* 59: 312-326, 2002.
58. **Bell CC, Han V, and Sawtell NB**. Cerebellum-like structures and their implications for cerebellar function. *Annual review of neuroscience* 31: 1-24, 2008.

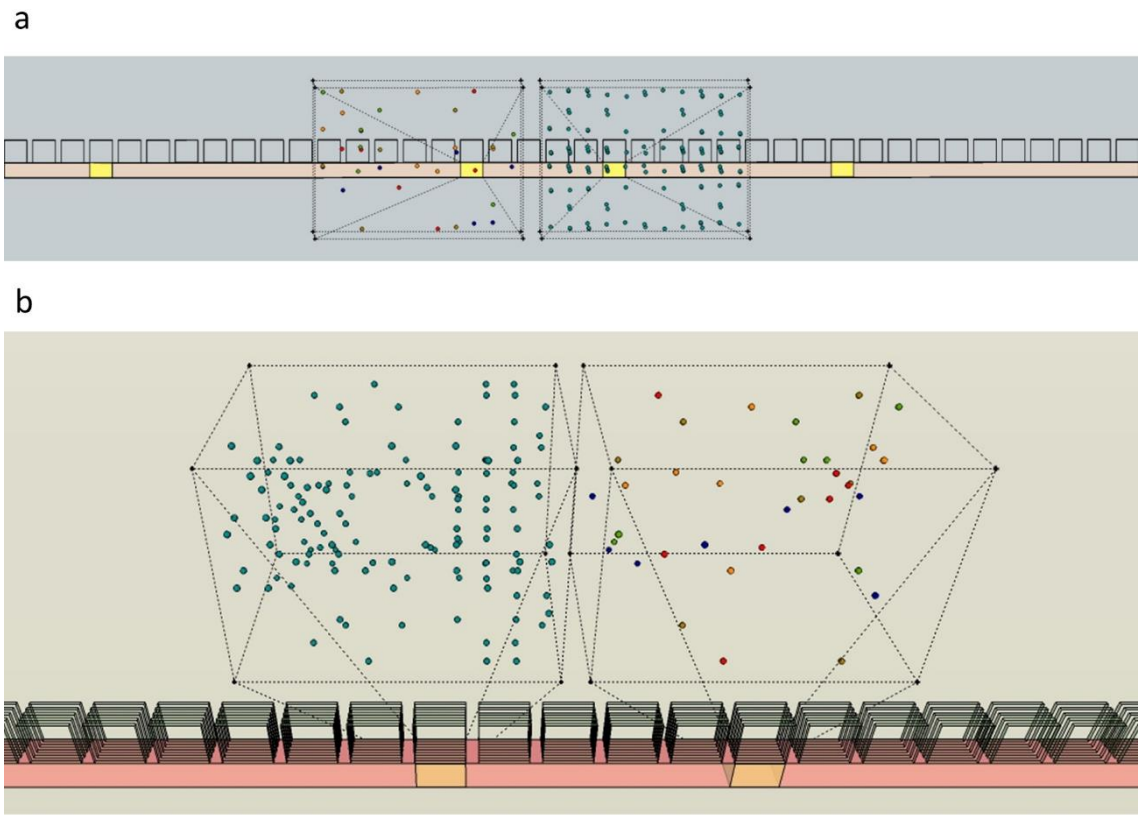

Fig 1 Mossy fibres terminate in a row of randomly-spaced clusters

a A schematic of a section of a straightened out microzone in vertical cross-section, i.e., perpendicular to the cerebellar surface, showing an exploded view of two fields. The row of squares represents the molecular layer. The pink region represents the granular layer. Mossy fibres give rise to clusters of terminals in the granular layer. The yellow regions represent field-sized locations of a sagittally-aligned row of terminal clusters to which a single mossy fibre might give rise. The section of a microzone shown here is the length of about 40 fields – a microzone is 75-100 fields long. **b** Mid-section of the same schematic from a rear view and with perspective added. Each of

the squares in (a) is now revealed by the viewing angle to be a row, 5 deep – cells in the molecular layer are severely flattened in the sagittal plane. The (in this view) right box shows randomly distributed terminals of 5 mossy fibres (each a different colour). We estimate that ∼180 mossy fibres contribute terminals to a field, and a field contains a total of around 700 terminals. Proportions of terminal size to field size are preserved. The left box shows terminals of 20 mossy fibres, also randomly distributed.

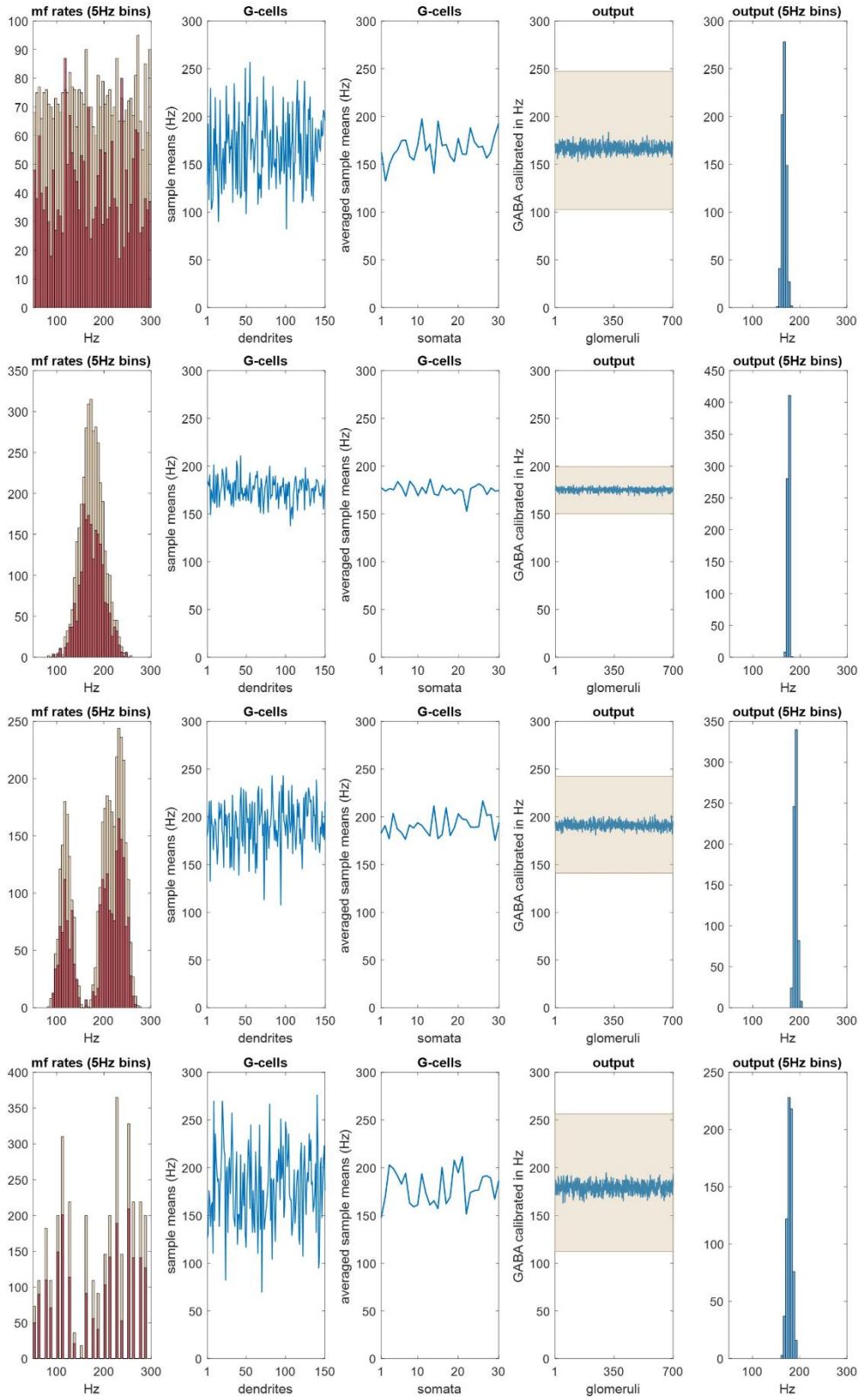
mf rates (5Hz bins)
Hz
G-cells
sample means (Hz)
dendrites
G-cells
averaged sample means (Hz)
somata
output
GABA calibrated in Hz
glomeruli
output (5Hz bins)
Hz

Fig 2 Golgi cell ensemble conversion

Column 1 We randomly generated (3,645) mossy fibre rates with a uniform, normal, twin-peaked or discontinuous distribution representing input to a row of 100 fields. Rates were randomly sampled to represent input to individual fields and copies added to reflect variable size of terminal clusters and that most clusters straddle field boundaries. Red data represent copies-included signals received by a row of three fields. **Column 2** The first-column red data were randomly sampled 150 times, sample size 4, representing mossy fibre input to a 3-field population of 30 Golgi cells, each with 5 basal dendrites (and each of those receiving contact from 4 mossy fibres). Data are the sample means, representing dendritic depolarisation. **Column 3** Column 2 data were randomly divided into 30 groups of 5, representing 30 Golgi cells, each with 5 basal dendrites. Data are the means, representing somatic integration. **Column 4** We then took 700 random samples of column 3 data, sample size 8–12, reflecting convergent input from 3 fields of Golgi cells onto 700 glomeruli in the middle field (to which a three-field ensemble has output). Data are the sample means. **Column 5** The column 4 data are presented as a histogram.

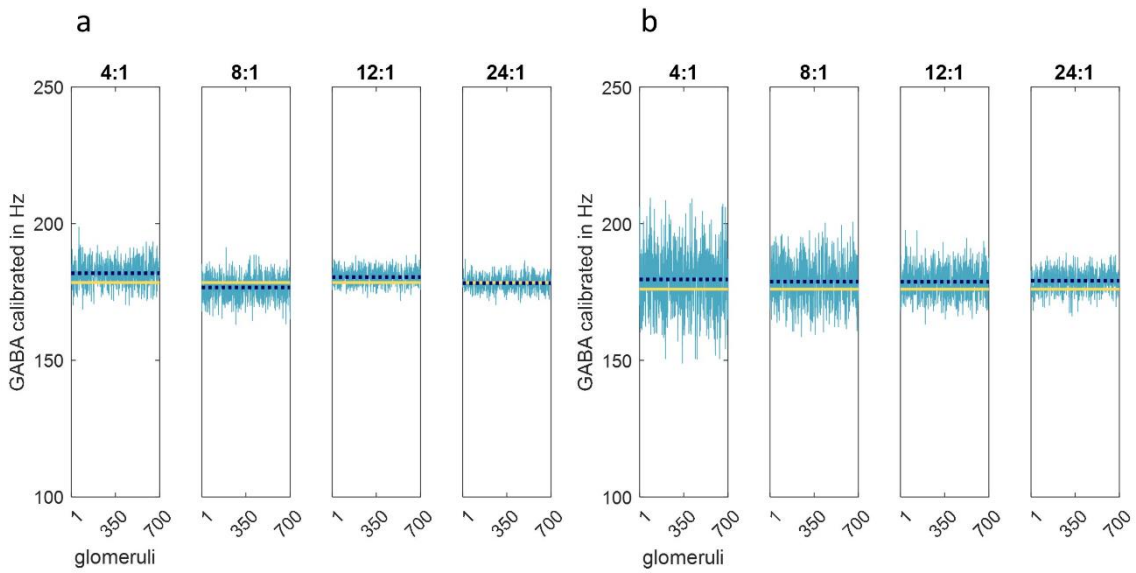

Fig 3 Unreported parameters: artificial refinements of the ensemble mechanism have a diminishing return and never eliminate random variability

Data were generated in the same way as Fig 2 column 4 with the row 4 distribution of mossy fibre rates (intended to be hypothesis neutral); y axes cover a shorter range than Fig 2 – 150 Hz vs 300 Hz – to bring out the vertical spread of the data. Yellow line: the mean of mossy fibre input rates to 3 fields; broken blue line: the glomerulus field mean. **a** We varied the convergence ratio of mossy fibres onto Golgi cell basal dendrites. The convergence ratio is shown above each panel. Other parameters are fixed. **b** We varied the number of Golgi cells with convergent input to a glomerulus (the ratios are again above each panel). Both are unknowns, as far as we know. A narrower range represents tighter within-field synchrony of the rate threshold. Note that in both cases increasing the ratio above 12:1 makes little further difference.

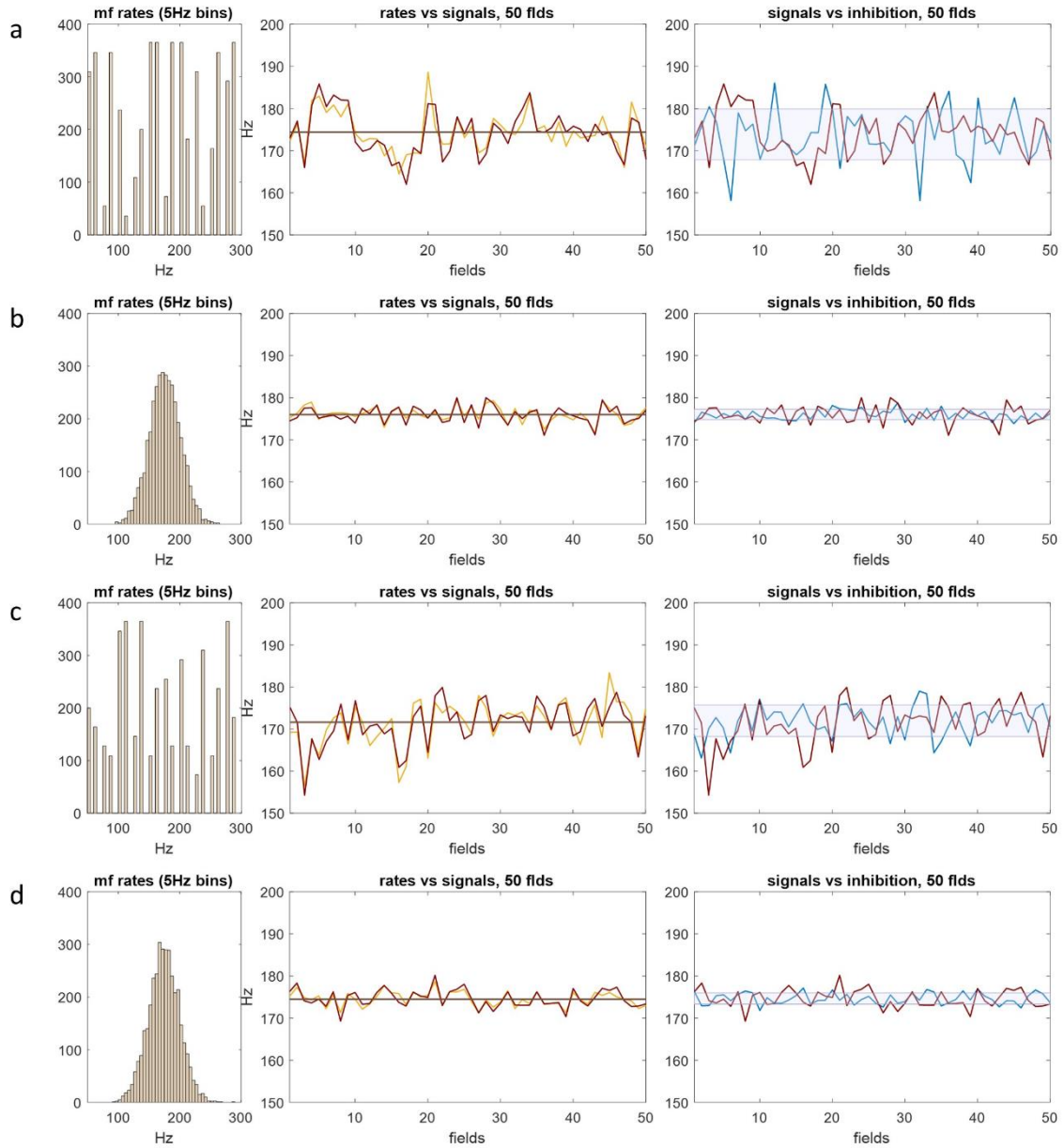

Fig 4 Output of the ensemble conversion is synchronised along a row of fields

Left column. Randomly generated values representing mossy fibre firing rates received by a row of 100 fields. **Middle column**. Brown line: mean of the left-column data; yellow line: the mean of rates received by each field; red line: the mean of rates with

copies added to reflect mossy fibre terminal clustering (so, the mean of all signals, including duplicate rates). Adding copies has little effect on the mean of input rates to a field. **Right column**. Blue line: the glomerulus field means; shaded area: SD; red line: a copy of the red data in column two. Both are statistically constrained to range that is proportional to variance of the sampled distribution (left column data), and have the same mean. The range can be narrow. Within that range, they vary at random and independently. Variation is not compounded, that is, layers of random sampling do not have a cumulative effect. In the middle and right columns, y axes have a shorter range than Fig 2, 150–200 Hz, and 50 fields are shown (out of 100 simulated), to aid visualisation.

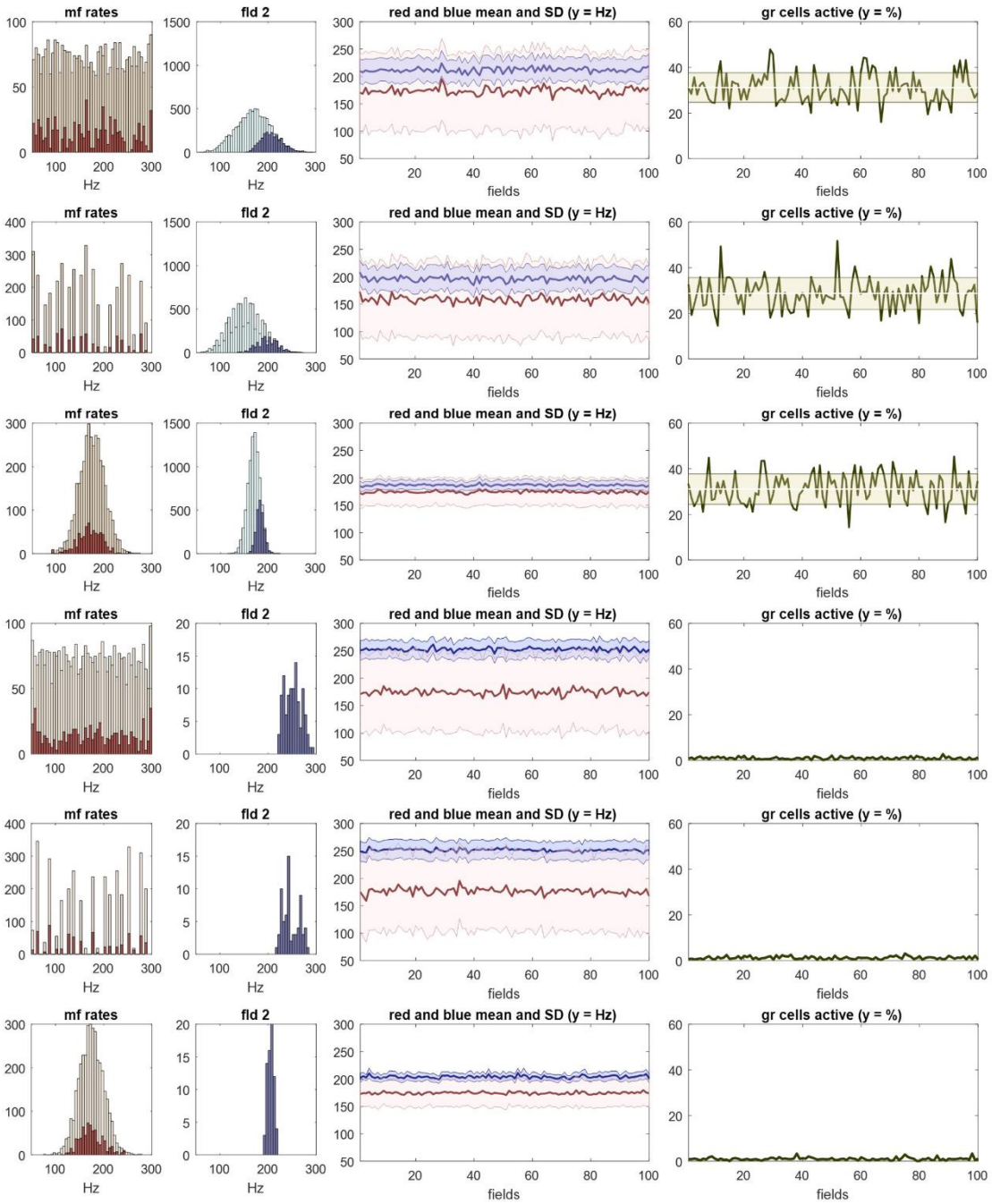
mf rates
fld 2
red and blue mean and SD (y = Hz)
gr cells active (y = %)
Hz
fields

Fig 5 Collective parameters of mossy fibre rates precisely predict the frequency distribution of granule cell rates in a row of fields

We incorporated the Golgi cell ensemble conversion into a simulation of recoding in the granular layer. **Column 1.** We randomly generated (3,645) mossy fibre rates with a uniform, discontinuous or normal distribution representing input to a row of 100 fields. Red data are rates received by a single field (field 2), with copies added, as an example. y axes are scaled to the data. **Column 2.** Red data for each field were randomly sampled 8,750 times, sample size 4, representing a per field population of 8,750 granule cells, each with 4 dendrites, which each receive contact from a single mossy fibre terminal. The field 2 sample means are displayed as a histogram (top three rows, pale green; there are the same number of green data in each panel). Blue data represent the smaller group of granule cells that fire (all rows). In the bottom three rows the group that fire is *much* smaller; y axes in the bottom three panels are rescaled. **Column 3.** The mean and SD of the red and blue data for all fields. **Column 4.** The percentage of granule cells that fire in each field. White line: mean; shaded area: SD (top three panels).

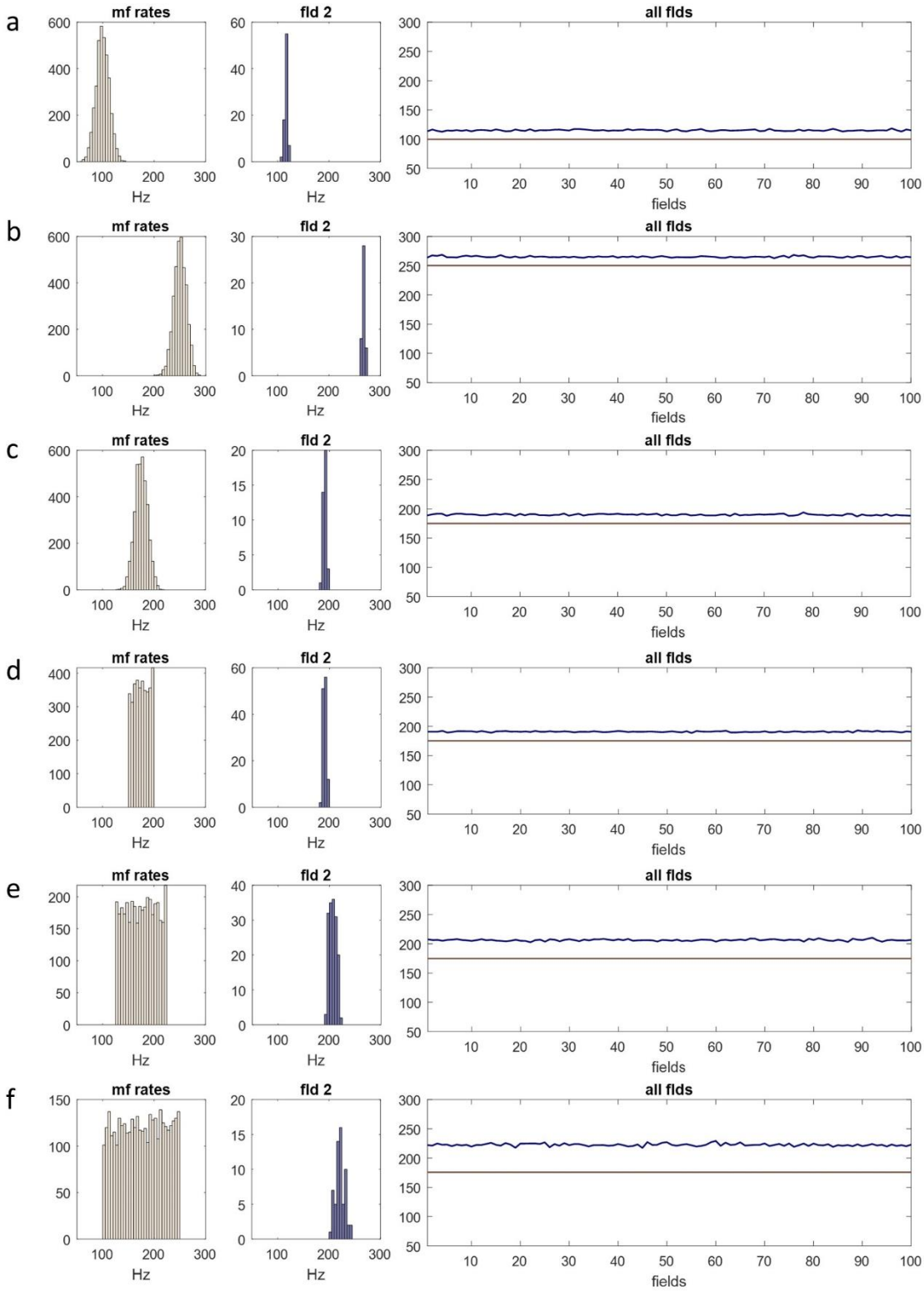
a
mf rates
fld 2
all flds
Hz
fields
b
mf rates
fld 2
all flds
Hz
fields
c
mf rates
fld 2
all flds
Hz
fields
d
mf rates
fld 2
all flds
Hz
fields
e
mf rates
fld 2
all flds
Hz
fields
f
mf rates
fld 2
all flds
Hz
fields

Fig 6 A linear relationship of mossy fibre rate parameters with the mean of the granule cell frequency distribution

Column 1 We randomly generated (3,645) mossy fibre rates with either a normal (SD 12.5) or uniform distribution representing input to a row of 100 fields – the sampled distribution. **Column 2** The sample means – the mean of mossy fibre rates received by a granule cell – in a single field (randomly selected as an example), displayed as a histogram. The rate threshold is set to generate sparse code, as in Fig 5, bottom 3 rows. Data are only for the small fraction of granule cells which fire. **Column 3** Brown line: the mean of the tan data; blue line: GC field means (the mean of the sample means for each field, for cells which fire). The GC field means have a linear relationship with the mean of the sampled distribution, if the shape and variance of the sampled distribution are approximately fixed. In a–c, the GC field means precisely track the mean of mossy fibre rates at a fixed mean distance of 15 Hz (SD 1.21 Hz). There is also a linear relationship with the range of the sampled distribution, with other parameters fixed. In d–f, increasing the range causes the same relative increase in the mean distance at which GC field means track the mean of the sampled distribution.